Earthquake Engineering, Tenth World Conference © 1992 Balkema, Rotterdam. ISBN 90 5410 060 5

The construction of large earthquake by a superposition of small events

Kojiro Irikura
DPRI, Kyoto University, Japan

ABSTRACT: We discuss the physical bases of the empirical Green's function method. The method we propose here is to construct strong ground motion from large earthquake by superposing ground motions from small events to follow the ω-squared scaling law with a constant stress parameter. This method can be extended to cases deviating from the ω-squared model, i.e. different stress parameters between large and small events and multiple shocks. Successful simulation results are shown for 4 earthquakes with different magnitudes, M 3.9, M 5.0, M 6.0 and M 6.1, occurring in almost the same source area, which are aftershocks of the 1983 Akita-Oki earthquake(M 7.7). Even if the small events used as the empirical Green's functions are not small enough to assume a point source solution, we obtain the synthetic seismograms fitting to the observed ones. This means the empirical Green's function is not simply substituted for the theoretical Green's function, but the simulation process by itself puts the rupture process on the fault plane into practice. The process of superposing small events to construct large earthquake may correspond to rupture-growing process to larger cracks by uniting small cracks.

1. Introduction

One of the most reliable method for predicting strong ground motion from large earthquake is the empirical Green's function method. The idea of the empirical Green's function was originally introduced by Hartzell(1978). Irikura(1983,1986) combined it with the scaling relations of source parameters and the scaling law of source spectra to obtain a deterministic formulation for the synthesis of the strong ground motion. The advantage of this method is to exploit not only the common propagation path and local site effects shared by small events and the target events , but also the source effects possessed by the small events within the fault area of the target event.

The original idea of the empirical Green's function method comes from using the records of small events instead of theoretical Green's function. From the above point of view, it is desirable that the small events should be as small as possible to be able to assume a point source solution in fault size. However, the smaller are events, the more difficult it is to obtain seismic records with enough accuracy. Therefore, most of simulations by the empirical Green's function methods have been made using not so small events as compared to the target events. For example, we had good simulation for strong ground motions from the 1980 Izu-Hanto-Toho-Oki earthquake using the records of the M 4.9 foreshock and also from the 1983 Akita-Oki earthquake with M= 7.7 using the seismic records of the M= 6.1 aftershock (Irikura, 1983, 1986).

In those simulations, the ground motions for the target events are obtained by superposing the records of small events in such a way as the synthetics follow the ω-squared spectral scaling model. We consider the above simulation process puts the rupture process of the fault plane into practice. This should be a reason that the simulated ground motions give a good agreement with the observed ones.

In this paper, detailed examinations of our method are made using broad-band records obtained by velocity strong motion seismometers from 4 earthquakes of different sizes (M 3.9, M 5.0, M 6.0, M 6.1), aftershocks of the 1983 Akita-Oki earthquake(M 7.7), occurring within a small area of several kilometers in diameter. By comparing the synthetics and the observed data, we discuss the physical basis of our simulation procedure.

2. Method of simulation

Here, we shall describe a procedure due to Irikura (1986) for constructing strong ground motion from large earthquake using small event records to follow the ω-squared scaling law with a constant stress parameter. The schematic illustration is shown in Fig. 1 (a). Let the moment of the target event be N^3 times that of the small event. We divide the fault plane into $N \times N$ elements. Then the subfault size is equivalent to the small event (hence-forth called subevent) if a constant stress condition is assumed between the large and small events.

The ground motion A(t) from the target event is expressed in terms of the ground motion a(t) from the subevent as follows:

$$A(t) = \sum_{i=1}^{N^3} (r/r_i) F_i(t) * a(t), \tag{1}$$

$$F_i(t) = \delta(t - t_i) + \frac{1}{n'} \sum_{j=1}^{(N-1)n'} \delta[t - t_i - \frac{(j-1)\tau}{(N-1)n'}], \tag{2}$$

and

$$t_i = r_i/V_c + \xi_i/V_R, \tag{3}$$

where r is the hypocentral distance from the observation point to the subevent, r_i is the distance from the observation point to the i-th fault element, ξ_i is the distance from the rupture nucleation point to the i-th fault element, V_R is the rupture speed, V_c is the seismic wave velocity under

consideration, τ is the rise time of the target event, n' is an appropriate integer to eliminate spurious periodicity (Irikura, 1983), and * represents the convolution. $F_i(t)$ is a filtering function to adjust a difference in slip time function between the target event and the subevent shown in Fig. 1 (b).

The above calculation results in N^3 times spectral level of the subevent at low frequencies due to coherent summation, assuring the correct moment. The high frequency spectral level , on the other hand, become proportional to the square root of N^2 times of the subevent due to incoherent summation, since F_i has asymptote to unity at high frequencies(Higher frequency range beyond $(N-1)n'/\tau$ must be excluded from consideration). Thus, the spectral amplitude at high frequencies will be proportional to the cube root of that at very low frequencies, meeting the condition for the ω-squared scaling law. The time-domain filter $F_i(t)$ described in the above equation is equivalent to the frequency-domain filter used by Boatwright (1988) for the same purpose. Physically, the filter mimics a case of rupture process over a heterogeneous fault simulated by Das and Aki (1977), in which a barrier on the fault plane eventually breaks slowly momentarily stopping the rupture as discussed later.

3. Simulation results

The aftershocks of the 1983 Akita-Oki earthquake were observed using strong motion velocity seismometers at FKR near the source area as shown in Fig. 2. The second and third largest aftershocks (M= 6.1 and M= 6.0) occurred close to each other near the southern edge of the mainshock fault plane. The two large aftershocks have similar source mechanisms from the push-pull distribution of P wave first motions, but different source time function from the analysis of teleseismic data, according to Izutani and Katagiri (1989). The observed velocity seismograms and the accelerograms by differenciating the velocity ones are used for synthesis from the above two events and other two smaller aftershocks (M= 5.0 and M= 3.9). Hence-forth, we call the M= 6.1, M= 6.0, M= 5.0, and M= 3.9 events, Event A, B, C and D, respectively. Event A, C, and D have relatively simple waveforms, while Event B has comparatively complex waveforms.

First, we synthesize ground motions from Event C (M= 5.0) using the records of Event D (M= 3.9). The moment ratio is estimated to be about 30, from the low frequency spectral levels of those two events. We find in (1) of Fig. 3 the synthetics agree well with the observed ones in acceleration as well as in velocity. The spectral ratio between the synthetic and observed one is almost flat except lower frequencies below 0.5 Hz. It is caused by poor signal levels from Event D in such low frequency range compared with background noise levels. This good agreement between the synthetic and the observed means that both event C and D just follow the ω-squared spectral scaling model.

Next we calculate the synthetic velocity and acceleration for event A (M= 6.1) using the records of event C (M= 5.0). The moment ratio is about 100. In this case, we need to pay attention to the difference in stress parameter between the target event and the subevent (Irikura, 1986). Event A has a stress parameter four times larger than Event C from the relation between moment and corner frequency. After correcting the difference of stress parameters, we obtained the synthetic motions of Event A from Event C records. We find in (2) of Fig. 3 the synthetics and the observed ones agree well each other both in velocity and acceleration.

Finally, we attempt to synthesize ground motion from Event B, probably expected to be a multiple-shock from complexity of the acceleration waveform. After trying forward modeling several times, we find this event consists of two shocks which have different source sizes and different stress parameters and occur at an interval of 2.1 sec. Not the records of Event C but those of Event D are appropriate to the empirical Green's function for Event B. We see in (3) of Fig. 3, the synthetics from such multi-shock agree well with the observed ones.

4. Discussion and Conclusions

The ground motions for large events are simulated by superposing the records of small events in such a way as the synthetics follow the ω-squared model. The synthetics from the above method show a good fitting to the broad-band observed records ranging from 0.1 to 10 Hz using seismic records by velocity strong motion seismometers from aftershocks (M3.9, M5.0, M 6.0, and M 6.1) of the 1983 Akita-Oki earthquake, occurring within a small area of several kilometers in diameter.

This synthetic process is not simple sum of ground motions from an aggregate of small cracks which cover the faulting area of the larger event. We cannot match both the high-frequency and low- frequency spectral amplitudes of the larger events expected from the ω-squared scaling by simply summing up small event records. Our synthesis makes a summation to match not only the moment at low frequencies but also spectral contents at high frequencies to keep stress-drop constant independent of source sizes. This method can be easily extended to cases having different stress parameters between small and large events and multiple events.

The physical model to generate the ω-squared spectral scaling is a single crack model. However, such crack model has a limitation to consider observed accelerograms. As shown in Fig. 4, the simple crack model generates basically only two pulses, even if crack becomes larger. This is unlikely to happen for large earthquakes. On the other hand, a multi-crack model generates a number of acceleration pulses, but seismic motions from the multi-crack source do not follow the ω-squared model. To obtain the seismic motions following the ω-squared model, barriers between cracks have to be eventually broken, once cracks stop at barriers. Das and Aki (1977) had the numerical simulation in the two-dimensional problem for the above model and confirmed the seismic generation of the ω-squared model.

The physical basis of this synthetic process may be explained as shown at several stages in Fig. 5. When some irregularities such as barriers or asperities, the crack propagation will be stopped remaining unbroken barriers and eventually such barriers will be broken because of subsequent increase in dynamic stress. The ground motion from this process have the spectral contents expected from the ω-squared model.

REFERENCES

Boatwright, J. 1988. The seismic radiation from composite models of faulting. Bull. Seism. Soc. Am. 78, 489-508.

Das, S., and K. Aki. 1977. Fault plane with barriers: a versatile earthquake model. J. Geophys. Res., 82, 5658-5670.

Hartzell, S. H. 1978. Earthquake aftershocks as Green's functions, Geophys. Res. Lett., 5, 1-4.

Irikura, K. 1983. Semi-empirical estimation of strong ground motions during large earthquakes, Bull. Disas. Prev. Res. Inst., Kyoto Univ. 33, 63-104.

Irikura, K. 1986. Prediction of strong acceleration motions using empirical Green's function, Proc. 7th Japan earthquake engineering, 151-156.

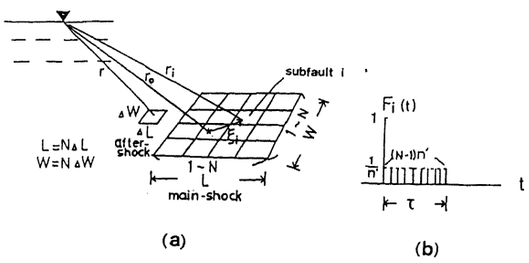

Fig. 1. (a) Schematic illustration of the Green's function method. The fault areas of the mainshock and a small event (aftershock) are defined to be $L \times W$ and $\Delta L \times \Delta W$, respectively. (b) $F_i(t)$, a filtering function to adjust a difference in slip time function between the mainshock and the small event.

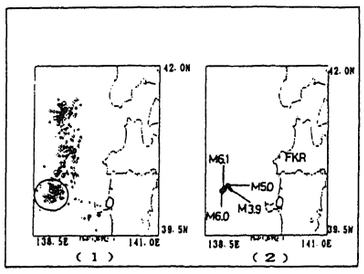

Fig. 2. (1) Epicentral distribution of aftershocks of the 1983 Akita-Oki earthquake and (2) Epicenters of the aftershocks (event A: M6.1, event B: M6.0, event C: M5.0, event D: M3.9) analyzed in this study (Ishikawa et al., 1985; Ishikawa, 1986; and JMA data).

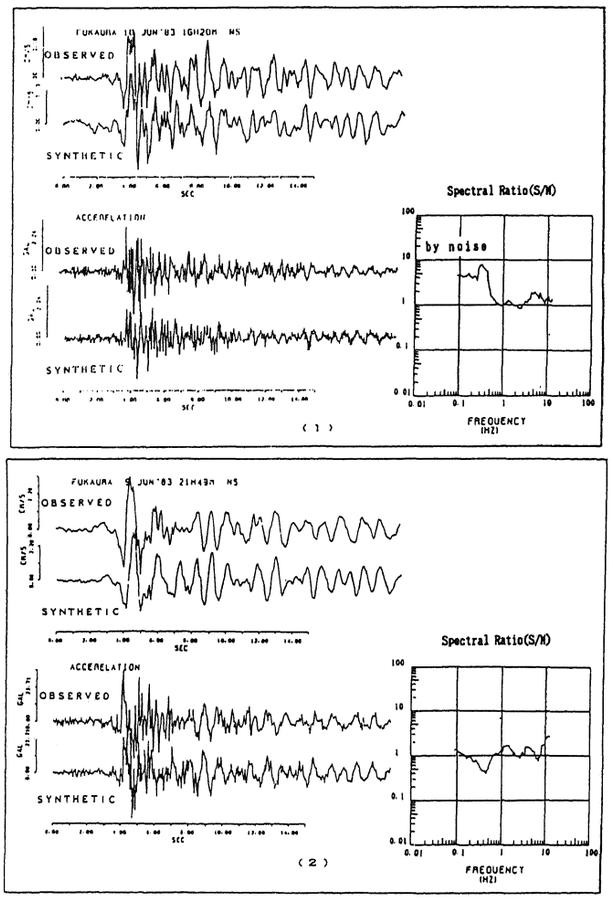

Fig. 3. Comparison between observed and synthetic seismograms. (1) Synthesis of event C (M5.0) using event D (M3.9) as empirical Green's function. (2) Synthesis of event A (M6.1) using event C (M5.0) as empirical Green's function. (3) Synthesis of event B (M6.0) using event D (M3.9) as empirical Green's function. In (1) to (3), each upper left shows velocity seismograms, each lower left shows accelerograms, and each right shows spectral ratio (synthetic/observed). In (1), the increase of the ratio at frequencies lower than 0.5 Hz is caused by the noises included in the record of event D (M3.9) used as empirical Green's function.

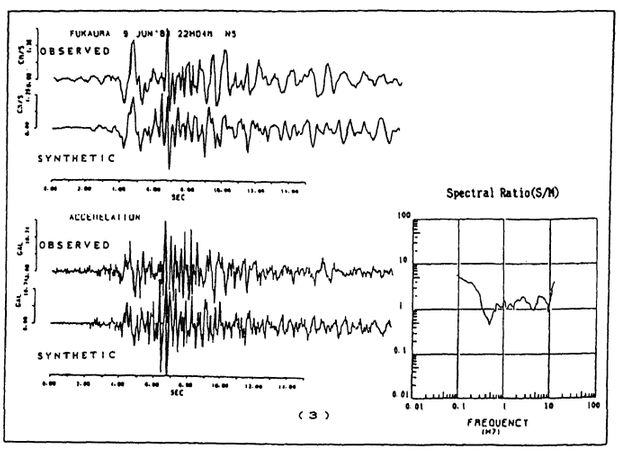

Fig. 3. (Continued)

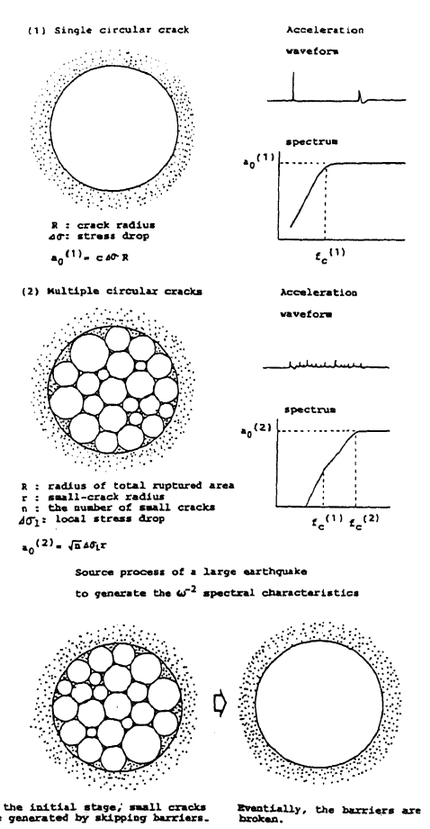

Fig. 4. Illustration for source process of large earthquake to generate the ω-squared spectral characteristics.

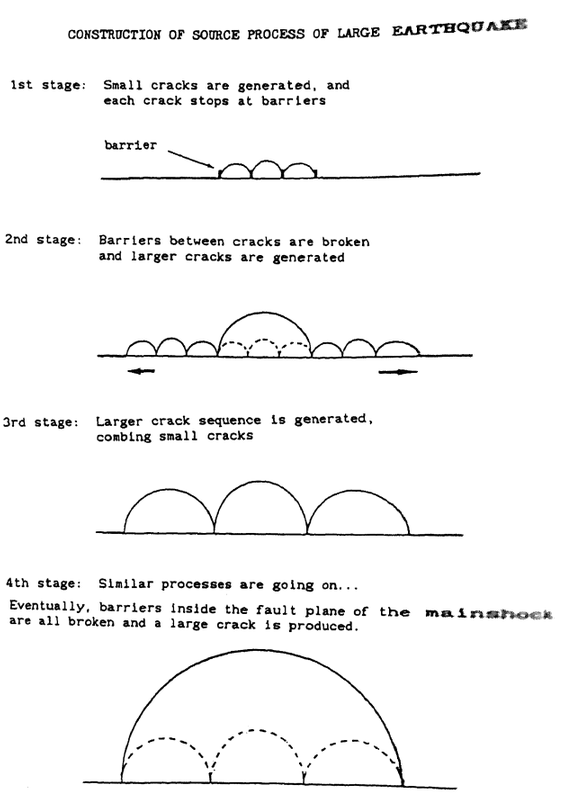

Fig. 5. Construction of source process of a large earthquake.